

Flat Band Josephson Junctions with Quantum Metric

Zhong C.F. Li^{1,*}, Yuxuan Deng^{1,*}, Shuai A. Chen^{1,†}, Dmitri K. Efetov², and K. T. Law^{1‡}

1. Department of Physics, Hong Kong University of Science and Technology, Clear Water Bay, Hong Kong, China and
2. Fakultät für Physik, Ludwig-Maximilians-Universität, Schellingstrasse 4, München 80799, Germany

In this work, we consider superconductor/flat band material/superconductor (S/FB/S) Josephson junctions (JJs) where the flat band material possesses isolated flat bands with exactly zero Fermi velocity. Contrary to conventional S/N/S JJs in which the critical Josephson current vanishes when the Fermi velocity goes to zero, we show here that the critical current in the S/FB/S junction is controlled by the quantum metric length ξ_{QM} of the flat bands. Microscopically, when ξ_{QM} of the flat band is long enough, the interface bound states originally localized at the two S/FB, FB/S interfaces can penetrate deeply into the flat band material and hybridize to form Andreev bound states (ABS). These ABS are able to carry long range and sizable supercurrents. Importantly, ξ_{QM} also controls how far the proximity effect can penetrate into the flat band material. This is in sharp contrast with de Gennes' theory for S/N junctions in which the proximity effect is expected to be zero when the Fermi velocity of the normal metal is zero. We further suggest that the S/FB/S junctions gives rise to a new type of resonant Josephson transistors which can carry sizeable and highly gate-tunable supercurrent.

Introduction.—The study of flat band superconductors had attracted much attention in recent years due to the discovery of superconducting moiré materials with flat bands [1–23]. One interesting property of flat band superconductors is that the superfluid weight is not zero but proportional to the quantum metric [24–26] of the flat band despite the vanishing Fermi velocity [27]. This finding inspired a large number of studies on the superfluid weight of flat band superconductors [10, 28–44]. More recently, it was realized that the quantum metric defines an important electronic length scale in flat band materials called the quantum metric length ξ [45]. In particular, ξ determines the superconducting coherence length, which is expected to be zero for flat band superconductors according to BCS theory [22, 45]. Linking the superconducting coherence length with ξ [22, 45] explained the observed long superconducting coherence length in twisted bilayer graphene [21], which deviates greatly from what the BCS theory predicted.

As the superconducting coherence length generally controls the sizes of electronic objects in superconductors, we expect that ξ also governs the sizes of electronic objects such as Andreev bound states (ABS), Yu-Shiba states in flat band materials. In this work, we verify this speculation and demonstrate how the quantum metric can control the ABS size at the weak link of the superconductor/flat band material/superconductor (S/FB/S) Josephson junctions (JJs). Furthermore, we show that the superconducting proximity effect can penetrate deeply into the flatband material and the decay length is controlled by the quantum metric length, which can be orders of magnitude longer than the lattice length scale. Our results are in sharp contrast to de Gennes' theory of superconductor/normal metal (S/N) junctions which predicts that the superconducting proximity effect into a flat band should be zero [46, 47].

In the rest of this work, we first use with a one dimen-

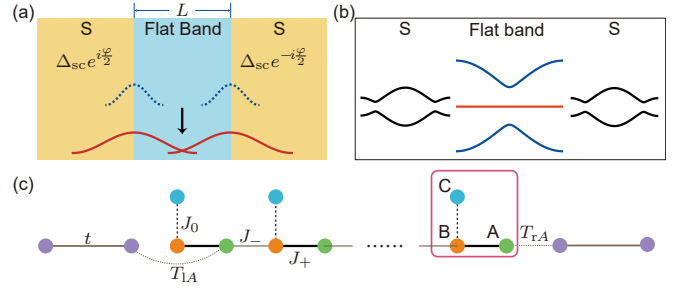


FIG. 1. (a) A schematic illustration of a S/FB/S junction. The blue dashed lines denotes two interface states in the small quantum metric regime. When quantum metric increases, the two interface states hybridize with each other to form ABS at the junction as denoted by the solid red curves. (b) The schematic band structure of the flat band material and the superconducting leads. We assume an isolated flat band (red line) near the Fermi energy of the JJ. (c) The lattice model of the JJ. The flat band is described by a Lieb lattice with three lattice sites per unit cell. The superconducting leads couple to the nearest A-sites of the Lieb lattice with coupling strengths T_{1A} and T_{rA} respectively. The purple dots represent sites of the superconducting leads.

sional model to illustrate the properties of S/FB/S junctions (as schematically shown in Fig. 1(a) and (b)) and the conclusions can be easily generalized to two dimensions. First, we build a model to describe the junction where the weak link is a 1D Lieb lattice [48–51] which possesses a pair of spin degenerate flat bands and tunable quantum metric. The Lieb lattice model is illustrated in Fig. 1(c). We define a quantum metric length ξ_{QM} for the 1D Lieb model. Second, when the Lieb lattice is coupled to two superconductors and when the quantum metric is small, two interface states (denoted by blue dashed lines) are created at the S/FB and FB/S interfaces as shown in Fig. 1(a). Third, when the quantum metric increases, ξ_{QM} increases and the interface states penetrate deeper

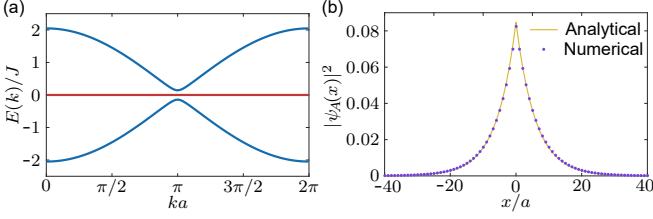


FIG. 2. (a) The energy spectrum of a 1D Lieb lattice. The flat band (in red) is separated from the dispersive bands by δJ . The parameters of the model are: $J = 10^4 \Delta_{\text{sc}}$, $\delta = 0.03$. The superconducting gap $\Delta_{\text{sc}} = 1$ is set to be the energy unit for later discussions. (b) The probability distribution of the A-component of the bound state wavefunction $|\psi_A(x)|^2$ localized near $x = 0$ for a Lieb lattice with a local potential perturbation at $x = 0$. This decay length of this bound state is well-fitted by the analytical expression of $\psi_A(x) \propto \exp(-|x|/8\xi_{QM})$.

into the bulk of the Lieb lattice as the decay length of the interface state is controlled by ξ_{QM} . When ξ_{QM} is comparable with the junction length, the two interface states hybridize to form two ABS (illustrated by the red solid lines in Fig. 1(a)). As a result, the energy levels of these ABS are sensitive to the phases of the superconductors so that they can carry supercurrents. Finally, we show that the critical Josephson current is sizable and highly gate-tunable even for long junctions and such S/FB/S JJs are new types of resonant Josephson transistors [52–56].

Quantum metric length ξ_{QM} of Lieb lattice— To start, we first focus on the Lieb lattice which describes the weak link of the flat band JJ. The Lieb lattice model possesses two isolated, spin degenerate, flat bands near the Fermi energy as depicted in Fig. 1(b) and 2(a). The Lieb lattice model has three sites per unit cell, labeled as A, B and C sites respectively [see Fig. 1(c)]. The Hamiltonian can be written as:

$$H_{\text{Lieb}} = \sum_{i\sigma} (J_+ a_{iA\sigma}^\dagger a_{iB\sigma} + J_0 a_{iC\sigma}^\dagger a_{iB\sigma} + J_- a_{i-1A\sigma}^\dagger a_{iB\sigma} + h.c.) - \sum_{\alpha i\sigma} \mu_N a_{i\alpha\sigma}^\dagger a_{i\alpha\sigma}. \quad (1)$$

Here, $J_\pm = J(1 \pm \delta)$, $J_0 = \delta J$, α is the orbital index, μ_N is the chemical potential. The flat band of the Lieb lattice in Eq. (1) is separated from the other two dispersive bands by an energy gap $J\delta$. The lattice constant is a which is set to be unity.

It is important to note that there is a lack of natural electronic length scale for the flat bands as the length scales associated with k_F and v_F are either not well-defined or zero. In the following, we show how the quantum metric length of the 1D Lieb lattice ξ_{QM} governs the decay length of bound states near the flat band energy of the Lieb lattice. To find ξ_{QM} , we start with the Bloch Hamiltonian of the Lieb lattice $h(k)$ (with the spin index omitted) and the Bloch states of the flat band $|u_0(k)\rangle$

which can be written as:

$$h(k) = 2J \begin{pmatrix} 0 & a_k & 0 \\ a_k^* & 0 & b_k \\ 0 & b_k^* & 0 \end{pmatrix}, |u_0(k)\rangle = \begin{pmatrix} \frac{b_k}{\sqrt{|a_k|^2 + |b_k|^2}} \\ 0 \\ -\frac{a_k^*}{\sqrt{|a_k|^2 + |b_k|^2}} \end{pmatrix}, \quad (2)$$

respectively. Here, $a_k = \cos(\frac{ka}{2}) + i\delta \sin(\frac{ka}{2})$ and $b_k = i\delta$. For the 1D Lieb lattice, the real part of the quantum metric tensor associated with the flat band [24] can be simplified as $g^0(k)$ such that

$$g^0(k) = \text{Re} \langle \partial_k u_0(k) | (1 - |u_0(k)\rangle \langle u_0(k)|) | \partial_k u_0(k) \rangle. \quad (3)$$

With $g^0(k)$, the quantum metric length of the Lieb lattice is:

$$\xi_{QM} = \int_{-\pi/a}^{\pi/a} g^0(k) \frac{dk}{2\pi}. \quad (4)$$

For the Lieb lattice, and for small δ , we have $\xi_{QM} = \frac{a}{16\sqrt{2}\delta}$ where δ tunes the coupling strength between the C-sites and the B-sites in the Lieb lattice. It is important to note that the Lieb lattice only involves nearest neighbor hopping but ξ_{QM} can be much larger than a . For example, with $\delta = 0.01$, ξ_{QM} is about $4.4a$. In the following, we show that ξ_{QM} dictates the size of the bound states which have energy near the flat band energy. For example, we introduce a single impurity at position $x = 0$ at site A of the Lieb lattice to trap a bound state. It is shown in the Supplemental Materials (SM) [57] that the bound state wavefunction $\psi_A(x)$, which is localized near $x = 0$, can be written as:

$$\psi_A(x) \approx \sum_k e^{ikx} |u_A(k)|^2 \propto \exp(-|x|/8\xi_{QM}). \quad (5)$$

Here, $u_A(k) = b_k / \sqrt{|a_k|^2 + |b_k|^2}$ is the first (A-site) component of $|u_0(k)\rangle$ and the decay length $8\xi_{QM}$ is determined by the complex poles of $|u_A(k)|^2$. Since the decay length generally depends on the wavefunctions of the flat band, we expect that the factor of 8 is model dependent. A bound state wavefunction calculated numerically is shown in Fig. 2(b). Incredibly, the analytical solution in Eq. (5), with $\xi_{QM} = \frac{a}{16\sqrt{2}\delta}$, matches the numerical results of Fig. 2(b) extremely well and it clearly demonstrates that the size of the bound state wavefunction is controlled by ξ_{QM} . The more general bound state solutions of the Lieb lattice are presented in the SM [57]. Importantly, as shown below, the ABS sizes of a flat band JJ are also governed by ξ_{QM} which determines the JJ properties.

Interface states of flat-band JJs.— In this section, we study a flat band JJ depicted in Fig. 1(a). The left (L) and right (R) leads are set to be conventional s-wave superconductors described by the Hamiltonians H_L and

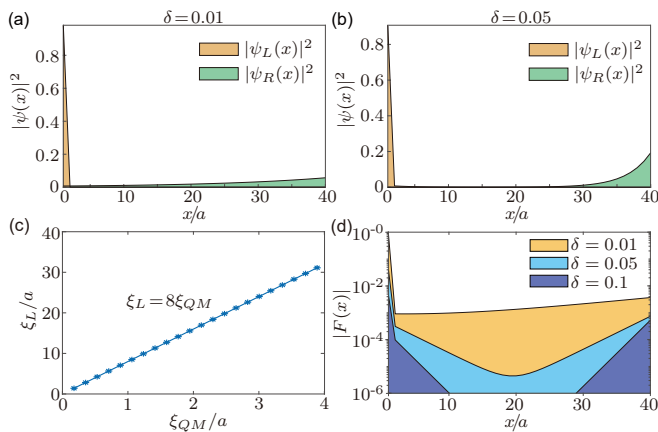


FIG. 3. Probability distribution of the interface states $\Psi_L(x)$ and $\Psi_R(x)$ (a) $\delta = 0.01$ and (b) $\delta = 0.05$. The wavefunctions become more localized for larger δ . The junction length is set to be $L = 40$. The parameters of the Hamiltonian H_{JJ} are: $J = 10^4 \Delta_{sc}$, $t = 100 \Delta_{sc}$. (c) The decay length ξ_L of the interface states for different values of ξ_{QM} . The relation $\xi_L = 8\xi_{QM}$ was found both numerically and analytically. (d) The pairing correlation $|F(x)| = |\sum_{\alpha} \langle a_{x\alpha\uparrow}^{\dagger} a_{x\alpha\downarrow}^{\dagger} \rangle|$ in log scale. $|F(x)|$ decays exponentially into the bulk for large δ . When δ is small, which corresponds to large ξ_{QM} , the pairing correlation can penetrate deeply into the bulk of the weak link.

H_R , respectively, where

$$H_{L/R} = \sum_{\langle ij \rangle \sigma} -(t + \mu_s \delta_{ij}) c_{i\sigma}^{\dagger} c_{j\sigma} + \sum_i (\Delta_{l/r} c_{i\uparrow}^{\dagger} c_{i\downarrow}^{\dagger} + h.c.). \quad (6)$$

Here, $\langle ij \rangle$ denotes the hopping between the nearest neighbor sites, $\sigma = \uparrow\downarrow$ is the spin indice and μ_s is the chemical potential. The chemical potential is set to be $\mu_s = \mu_N = 0$ in this section so that the flat band energy is tuned to the Fermi energy of the superconducting leads. The pairing potentials of the two leads are denoted by $\Delta_{l/r} = \Delta_{sc} e^{\pm i\varphi/2}$ where φ denotes the phase difference between the two superconductors and Δ_{sc} is a constant.

The couplings between the superconducting leads and the Lieb lattice (modelled by Eq. (1)) is described by the coupling Hamiltonian H_c

$$H_c = \sum_{\alpha\sigma} (T_{l\alpha} c_{l\sigma}^{\dagger} a_{r\alpha\sigma} + T_{r\alpha} c_{r\sigma}^{\dagger} a_{l\alpha\sigma} + h.c.), \quad (7)$$

where $T_{l/r,\alpha}$ labels the coupling between the left/right superconducting lead with the nearest A -site of the Lieb lattice (See Fig. 1(c)). Coupling to other sites will only change the results quantitatively.

The total Hamiltonian of the one-dimensional flat band JJ can be written as $H_{JJ} = H_R + H_L + H_{Lieb} + H_c$. In conventional S/N/S JJs, the critical supercurrent as well as the superconducting proximity effect are expected to be zero when the Fermi velocity of the normal metal goes to zero [47, 58]. In the following, we demonstrate how

an ABS which spreads across the JJ can emerge when the quantum metric length ξ_{QM} of the Lieb lattice is comparable with the junction length and these ABS can carry sizable and long range supercurrents. The pairing correlation can also penetrate deeply into the junction.

As depicted in Fig. 3(a), when the two superconducting leads are coupled to the Lieb lattice with flat bands, two interface states, $\Psi_L(x)$ and $\Psi_R(x)$ are created as schematically shown in Fig. 1(b). The states $\Psi_L(x)$ and $\Psi_R(x)$ are not degenerate with each other in general, but each of them is spin degenerate. These wavefunctions have six components due to the electron and hole contributions from the three orbitals (A, B and C orbitals) of the Lieb lattice. Physically, as the middle band of the Lieb lattice is exactly flat and the superconductor is gapped, when an interface state with energy away from the flat band energy is created, this state must be localized at the interface. Given that the energy of the state is also within the quasiparticle gap of the superconducting leads. The question is, what is the localization lengths of these interface states? According to de Gennes' theory of proximity effect [46, 47], the localization length of the bound states should be zero because of the zero Fermi velocity of the flat bands.

To answer this question, we recall that the quantum metric length determines the superconducting coherence length of flat band superconductors [22, 45]. It is reasonable to speculate that ξ_{QM} should be related to the localization lengths of the bound states and this is indeed the case. Fig. 3(a)-(b) depict $|\Psi_L(x)|^2$ and $|\Psi_R(x)|^2$ at the flat band JJ with two different values of δ , respectively. Even though the two interface states look very different from each other as the details of the wavefunctions depend on the details of the interfaces, the localization lengths of the wavefunctions (on the Lieb lattice side) are the same and controlled by ξ_{QM} . Fig. 3(c) depicts the localization lengths ξ_L of the two interface states as a function of ξ_{QM} . The localization length of the interface states is extracted by assuming that the wavefunction inside the weak link has a form $\Psi_{L/R}(x) \propto e^{-|x|/\xi_L}$, where x is measured from the S/FB or FB/S interfaces. It is clear from Fig. 3(c) that the numerically extracted localization length of the interface states is $\xi_L = 8\xi_{QM}$ where $\xi_{QM} = a/(16\sqrt{2}\delta)$. This is the same decay length found in Eq. (5), and analytical results are given in SM [57].

Importantly, when the ξ_{QM} is comparable with the junction length, the two interface states hybridize into two ABS which spread across the weak link region. In this case, there is pairing correlation across the whole weak link. The pairing correlation is defined as $|F(x)| = |\sum_{\alpha} \langle a_{x\alpha\uparrow}^{\dagger} a_{x\alpha\downarrow}^{\dagger} \rangle|$, where α is the orbital index. $F(x)$ inside the flat band material can be easily extracted from the Green's function $G(E) = 1/(E - H_{JJ})$ in real space and the results are shown in Fig. 3(d). $F(x)$ with three different values of δ were demonstrated. It is clear that when ξ_{QM} is large, the superconducting proximity effect

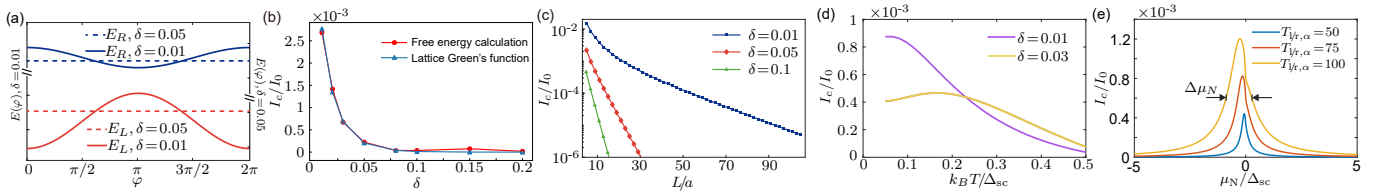


FIG. 4. (a) The energy-phase relation of the ABS at the junction for $\delta = 0.01$ and $\delta = 0.05$, respectively. As δ increases, the bound state energy becomes insensitive against change of φ . At $\varphi=0$ and $\delta=0.01$, the energy of the levels are: $E_R = -0.28\Delta_{sc}$ and $E_L = -0.97\Delta_{sc}$. While at $\delta=0.05$, $E_R = -0.98\Delta_{sc}$ and $E_L = -0.99\Delta_{sc}$. (b) The critical current as a function of δ with $L = 10a$. The results obtained from the free energy calculations and lattice Green's functions agree with each other. (c) The critical current generally decays exponentially as the junction length L increases. (a)-(c) are calculated with temperature $T=0.1\Delta_{sc}$. (d) The critical current I_c as a function of temperature $k_B T$, for different choice of δ . The above figures are plotted using $T_{r/1,\alpha} = 10^2 \Delta_{sc}$ and $J = 10^4 \Delta_{sc}$. (e) The critical current $I_c(\mu_N)$ as a function of the chemical potential of the flat band, for different coupling strengths $T_{r/1,\alpha}$. The temperature is set at $k_B T = 0.01\Delta_{sc}$. The full width at half maximum, $\Delta\mu_N$, is proportional to $|T_{r/1,\alpha}^2|$.

can penetrate deeply into the bulk of the flat band material.

ABS and Josephson Currents— As shown in Fig. 3(c) and schematically illustrated in Fig. 1(a), when $\xi_L = 8\xi_{QM}$ is comparable with the junction length, the two interface states hybridize into two ABS which spread across the weak link. As a result, the energy levels of the ABS depend of phase difference of the two superconducting leads φ . Therefore, we expect a finite Josephson current $I = \frac{\partial F_{JJ}(\varphi)}{\partial \varphi}$ where $F_{JJ}(\varphi)$ is the free energy of the JJ. In Fig. 4(a), the energy of the ABS as a function of φ are shown. When ξ_{QM} is short compared with the junction length (large δ), the two interface states do not couple to each other and the bound state energies are insensitive to the change of φ (dashed lines in Fig. 4(a)). On the contrary, when ξ_{QM} is long (with small δ), the two interface states hybridize. In this case, the energies of the two ABS $E_{\pm}(\varphi)$ are φ dependent (solid lines) and finite Josephson currents emerge. The critical Josephson current at different values of the quantum metric length is depicted in Fig. 4(b). The Josephson currents in Fig. 4(b) are determined by numerically evaluating $F_J(\varphi)$ through exact diagonalization of a finite system. The same results are also obtained by the lattice Green's function approach [59, 60]:

$$I(\phi) = \frac{2e}{\hbar} k_B T \text{Im} \sum_{\omega_m} \text{Tr}(V_{n+1,n} G_{n,n+1}(i\omega_m) - V_{n,n+1} G_{n+1,n}(i\omega_m)), \quad (8)$$

where ω_m is Matsubara frequency, n is the index of lattice site, V encodes the hopping amplitudes between neighboring sites and $[G_{n,n+1}(i\omega_m)]_{\alpha\beta} = \langle n\alpha | G(i\omega_m) | n+1, \beta \rangle$ refers to the matrix element of the lattice Green's function $G(i\omega_m)$ of the entire Josephson junction with $G(i\omega_m) = (i\omega_m - H_{JJ})^{-1}$. The details can be found in SM [57].

The length dependence of the critical currents at three different quantum metric length is shown in Fig. 4(c). It

is important to note that for large ξ_{QM} , the critical current can be in the order of 10^{-2} to 10^{-3} of $I_0 = \frac{e\Delta_{sc}}{\hbar}$, which is the maximum Josephson current of a single conducting channel [61]. Interestingly, in our case, the large critical Josephson current can appear even if the band is exactly flat. This is one of the main results of this work. Furthermore, the temperature dependence of the Josephson current is shown in Fig. 4(d). It is interesting to note that the Josephson current is nonmonotonic as a function of temperature. This unexpected behavior can be easily understood by the out of phase energy-phase relations of the two ABS [See Fig 4(a)].

Resonant Josephson Transistor — The Josephson current calculated above assumes that the energy of the flat bands lies at the Fermi energy of the superconductors. In this section, we show that the critical Josephson current decreases dramatically once the flat band energy is gated away from the Fermi energy of the superconductors. The critical current as a function of the chemical potential of the Lieb lattice is determined by a Breit-Wigner transmission probability function [62] as shown in Fig. 4(e). It is clear from Fig. 4(e) that the critical Josephson current has a sharp resonance peak when the ABS energy matches the Fermi energy of the superconducting leads. Moreover, the full width at half maximum (FWHM) of the resonance peak is proportional to the amplitude of the coupling strength between the superconducting leads and the Lieb lattice such that $\Delta\mu \propto T_{r/1,\alpha}^2$. This sharp resonance allows a new design of resonant Josephson transistors [52, 53, 55, 56] in which a long range Josephson current is highly gate-tunable. Importantly, the theory discussed in this work applies to two-dimensional Lieb lattice mediated Josephson effect as well.

Discussion and Conclusion.— Before concluding, we would like to discuss a few points. First, the Lieb lattice is chosen to model the flat band material because the lattice is incredibly simple which only involves nearest neighbor hopping. At the same time, the model can

give rise to a very long ξ_{QM} which far exceeds the lattice length scale. This can avoid the complications induced by long range hopping. Second, the conclusion that the quantum metric can tune the critical Josephson current in S/FB/S junctions is generally true. We demonstrate the finite Josephson current with another flat band model in the SM [57]. Moreover, the Lieb lattice has an energy spectrum which closely resembles the case of twisted bilayer graphene (TBG) near magic angle [7]. Our S/FB/S junction results is highly relevant to S/TBG/S JJs which were fabricated experimentally [63–66]. We would like to point out that the flat band Josephson effect was studied previously in Ref. [36] but the quantum metric effect was not investigated.

To conclude, we show that the quantum metric, through the quantum metric length ξ_{QM} , plays an extremely important role in determining the properties of S/FB/S JJs. In sharp contrast with conventional S/N/S junctions in which the critical supercurrent is expected to be zero when the Fermi velocity of the normal metal goes to zero, there can be a large Josephson current in S/FB/S junctions which is tuned by the quantum metric. Also, we demonstrate that the superconducting proximity effect can penetrate deep into the weak link even when the Fermi velocity of the weak link is zero. This is also in sharp contrast to the well-established theory of de Gennes on superconducting proximity effects [46]. The understanding of S/FB/S JJs allows a new design of highly gate-tunable resonant Josephson transistors.

Acknowledgement— We thank Tai-Kai Ng, Adrian Po and A. Díez-Carlón for valuable discussions. K. T. L. acknowledges the support of the Ministry of Science and Technology, China and the Hong Kong Research Grants Council through Grants No. 2020YFA0309600, No. RFS2021-6S03, No. C6025-19G, No. AoE/P-701/20, No. 16310520, No. 16310219, No. 16307622, and No. 16309223.

* These authors contributed equally to this work.

† chsh@ust.hk

‡ phlaw@ust.hk

- [1] R. Bistritzer and A. H. MacDonald, Proceedings of the National Academy of Science **108**, 12233 (2011).
- [2] Y. Cao, V. Fatemi, S. Fang, K. Watanabe, T. Taniguchi, E. Kaxiras, and P. Jarillo-Herrero, Nature (London) **556**, 43 (2018).
- [3] Y. Cao, V. Fatemi, S. Fang, K. Watanabe, T. Taniguchi, E. Kaxiras, and P. Jarillo-Herrero, Nature (London) **556**, 43 (2018).
- [4] Y. Cao, V. Fatemi, A. Demir, S. Fang, S. L. Tomarken, J. Y. Luo, J. D. Sanchez-Yamagishi, K. Watanabe, T. Taniguchi, E. Kaxiras, R. C. Ashoori, and P. Jarillo-Herrero, Nature (London) **556**, 80 (2018).
- [5] X. Lu, P. Stepanov, W. Yang, M. Xie, M. A. Aamir, I. Das, C. Urgell, K. Watanabe, T. Taniguchi, G. Zhang, A. Bachtold, A. H. MacDonald, and D. K. Efetov, Nature (London) **574**, 653 (2019).
- [6] M. Yankowitz, S. Chen, H. Polshyn, Y. Zhang, K. Watanabe, T. Taniguchi, D. Graf, A. F. Young, and C. R. Dean, Science **363**, 1059 (2019).
- [7] H. C. Po, L. Zou, T. Senthil, and A. Vishwanath, Phys. Rev. B **99**, 195455 (2019).
- [8] E. Codecido, Q. Wang, R. Koester, S. Che, H. Tian, R. Lv, S. Tran, K. Watanabe, T. Taniguchi, F. Zhang, M. Bockrath, and C. N. Lau, Science Advances **5**, eaaw9770 (2019).
- [9] T. Hazra, N. Verma, and M. Randeria, Physical Review X **9**, 031049 (2019).
- [10] L. Balents, C. R. Dean, D. K. Efetov, and A. F. Young, Nature Physics **16**, 725 (2020).
- [11] J. S. Hofmann, E. Berg, and D. Chowdhury, Phys. Rev. B **102**, 201112 (2020).
- [12] P. Stepanov, I. Das, X. Lu, A. Fahimniya, K. Watanabe, T. Taniguchi, F. H. L. Koppens, J. Lischner, L. Levitov, and D. K. Efetov, Nature (London) **583**, 375 (2020).
- [13] E. Y. Andrei and A. H. MacDonald, Nature Materials **19**, 1265 (2020).
- [14] Y. Saito, J. Ge, K. Watanabe, T. Taniguchi, and A. F. Young, Nature Physics **16**, 926 (2020).
- [15] E. Y. Andrei, D. K. Efetov, P. Jarillo-Herrero, A. H. MacDonald, K. F. Mak, T. Senthil, E. Tutuc, A. Yazdani, and A. F. Young, Nature Reviews Materials **6**, 201 (2021).
- [16] V. Peri, Z.-D. Song, B. A. Bernevig, and S. D. Huber, Phys. Rev. Lett. **126**, 027002 (2021).
- [17] J. M. Park, Y. Cao, K. Watanabe, T. Taniguchi, and P. Jarillo-Herrero, Nature (London) **590**, 249 (2021).
- [18] N. Verma, T. Hazra, and M. Randeria, Proceedings of the National Academy of Science **118**, e2106744118 (2021).
- [19] H. M. Hastings and J. M. Daszkowski, Current Opinion in Solid State and Materials Science **25**, 100952 (2021).
- [20] P. Törmä, S. Peotta, and B. A. Bernevig, Nature Reviews Physics **4**, 528 (2022).
- [21] H. Tian, X. Gao, Y. Zhang, S. Che, T. Xu, P. Cheung, K. Watanabe, T. Taniguchi, M. Randeria, F. Zhang, C. N. Lau, and M. W. Bockrath, Nature (London) **614**, 440 (2023).
- [22] S. A. Chen and K. T. Law, Phys. Rev. Lett. **132**, 026002 (2024).
- [23] A. Daido, T. Kitamura, and Y. Yanase, arXiv e-prints , arXiv:2310.15558 (2023), arXiv:2310.15558 [cond-mat.supr-con].
- [24] J. P. Provost and G. Vallee, Communications in Mathematical Physics **76**, 289 (1980).
- [25] R. Cheng, arXiv e-prints , arXiv:1012.1337 (2010).
- [26] N. Marzari, A. A. Mostofi, J. R. Yates, I. Souza, and D. Vanderbilt, Rev. Mod. Phys. **84**, 1419 (2012).
- [27] S. Peotta and P. Törmä, Nature Communications **6**, 8944 (2015).
- [28] A. Julku, S. Peotta, T. I. Vanhala, D.-H. Kim, and P. Törmä, Phys. Rev. Lett. **117**, 045303 (2016).
- [29] M. Tovmasyan, S. Peotta, P. Törmä, and S. D. Huber, Phys. Rev. B **94**, 245149 (2016).
- [30] L. Liang, T. I. Vanhala, S. Peotta, T. Siro, A. Harju, and P. Törmä, Phys. Rev. B **95**, 024515 (2017).
- [31] P. Törmä, L. Liang, and S. Peotta, Phys. Rev. B **98**, 220511 (2018).
- [32] M. Tovmasyan, S. Peotta, L. Liang, P. Törmä, and S. D. Huber, Phys. Rev. B **98**, 134513 (2018).

- [33] X. Hu, T. Hyart, D. I. Pikulin, and E. Rossi, Phys. Rev. Lett. **123**, 237002 (2019).
- [34] F. Xie, Z. Song, B. Lian, and B. A. Bernevig, Phys. Rev. Lett. **124**, 167002 (2020).
- [35] A. Julku, T. J. Peltonen, L. Liang, T. T. Heikkilä, and P. Törmä, Phys. Rev. B **101**, 060505 (2020).
- [36] V. A. J. Pyykkönen, S. Peotta, P. Fabritius, J. Mohan, T. Esslinger, and P. Törmä, Phys. Rev. B **103**, 144519 (2021).
- [37] N. Verma, T. Hazra, and M. Randeria, Proceedings of the National Academy of Sciences **118**, e2106744118 (2021).
- [38] K.-E. Huhtinen, J. Herzog-Arbeitman, A. Chew, B. A. Bernevig, and P. Törmä, Phys. Rev. B **106**, 014518 (2022).
- [39] J. Herzog-Arbeitman, V. Peri, F. Schindler, S. D. Huber, and B. A. Bernevig, Phys. Rev. Lett. **128**, 087002 (2022).
- [40] T. Kitamura, A. Daido, and Y. Yanase, Phys. Rev. B **106**, 184507 (2022).
- [41] J. Herzog-Arbeitman, A. Chew, K.-E. Huhtinen, P. Törmä, and B. A. Bernevig, arXiv e-prints , arXiv:2209.00007 (2022).
- [42] K.-E. Huhtinen, J. Herzog-Arbeitman, A. Chew, B. A. Bernevig, and P. Törmä, Phys. Rev. B **106**, 014518 (2022).
- [43] P. Törmä, Phys. Rev. Lett. **131**, 240001 (2023).
- [44] M. Thumin and G. Bouzerar, Phys. Rev. B **107**, 214508 (2023).
- [45] J.-X. Hu, S. A. Chen, and K. T. Law, arXiv e-prints , arXiv:2308.05686 (2023).
- [46] P.-G. De Gennes, *Superconductivity of Metals and Alloys* (CRC press, 2018).
- [47] F. Tafuri, *Fundamentals and Frontiers of the Josephson Effect*, Vol. 286 (Springer Nature, 2019).
- [48] E. H. Lieb, Phys. Rev. Lett. **62**, 1201 (1989).
- [49] M. Niță, B. Ostahie, and A. Aldea, Phys. Rev. B **87**, 125428 (2013).
- [50] W.-X. Qiu, S. Li, J.-H. Gao, Y. Zhou, and F.-C. Zhang, Phys. Rev. B **94**, 241409 (2016).
- [51] M. R. Slot, T. S. Gardenier, P. H. Jacobse, G. C. P. van Miert, S. N. Kempkes, S. J. M. Zevenhuizen, C. M. Smith, D. Vanmaekelbergh, and I. Swart, Nature Physics **13**, 672 (2017).
- [52] C. Beenakker and H. Van Houten, in *Single-Electron Tunneling and Mesoscopic Devices: Proceedings of the 4th International Conference SQUID'91 (Sessions on SET and Mesoscopic Devices)*, Berlin, Fed. Rep. of Germany, June 18–21, 1991 (Springer, 1992) pp. 175–179.
- [53] D. D. Kuhn, N. M. Chtchelkatchev, G. B. Lesovik, and G. Blatter, Phys. Rev. B **63**, 054520 (2001).
- [54] A. A. Golubov, M. Y. Kupriyanov, and E. Il'ichev, Rev. Mod. Phys. **76**, 411 (2004).
- [55] E. V. Bezuglyi, E. N. Bratus', and V. S. Shumeiko, Phys. Rev. B **95**, 014522 (2017).
- [56] F. Wen, J. Shabani, and E. Tutuc, IEEE Transactions on Electron Devices **66**, 5367 (2019).
- [57] See Supplemental Material for: (i) Tight-Binding Model of Josephson Junction, (ii) Analytical Model, (iii) Quantum Metric Length as a Lower Bound, (iv) Supercurrent mediated by Bound States, (v) Supercurrent Calculation by Lattice Green's Function.
- [58] T. Klapwijk, Journal of superconductivity **17**, 593 (2004).
- [59] S. Datta, *Electronic Transport in Mesoscopic Systems*, Cambridge Studies in Semiconductor Physics and Microelectronic Engineering (Cambridge University Press, 1995).
- [60] A. Furusaki, Physica B: Condensed Matter **203**, 214 (1994).
- [61] C. W. J. Beenakker (2004) pp. cond-mat/0406127, arXiv:cond-mat/0406127 [cond-mat.mes-hall].
- [62] C. W. J. Beenakker, in *Transport Phenomena in Mesoscopic Systems*, edited by H. Fukuyama and T. Ando (Springer Berlin Heidelberg, 1992).
- [63] D. Rodan-Legrain, Y. Cao, J. M. Park, S. C. de la Barrera, M. T. Randeria, K. Watanabe, T. Taniguchi, and P. Jarillo-Herrero, Nature Nanotechnology **16**, 769 (2021).
- [64] F. K. de Vries, E. Portolés, G. Zheng, T. Taniguchi, K. Watanabe, T. Ihn, K. Ensslin, and P. Rickhaus, Nature Nanotechnology **16**, 760 (2021).
- [65] H. Sainz-Cruz, P. A. Pantaleón, V. o. T. Phong, A. Jimeno-Pozo, and F. Guinea, Phys. Rev. Lett. **131**, 016003 (2023).
- [66] J. Díez-Mérida, A. Díez-Carlón, S. Y. Yang, Y. M. Xie, X. J. Gao, J. Senior, K. Watanabe, T. Taniguchi, X. Lu, A. P. Higginbotham, K. T. Law, and D. K. Efetov, Nature Communications **14**, 2396 (2023).